Original Research

Revista Brasileira de Física Médica (2026) 20:912

Study and application of texture analysis to magnetic resonance images of patients with schizophrenia

G. F. Ricardo[1], R. V. Silveira[1,3], I. C. I. Carnielli[2], G. Castellano[1,3]

[1]Instituto de Física Gleb Wataghin, Universidade Estadual de Campinas, Campinas, Brazil
[2]Instituto de Matemática, Estatística e Computação Científica, Universidade Estadual de Campinas, Campinas, Brazil
[3]Brazilian Institute of Neuroscience and Neurotechnology, Campinas, Brazil

Abstract

Schizophrenia is a psychiatric disorder that affects more than 20 million people worldwide. However, the difficulty in diagnosing the disorder has led to the study and development of techniques to assist clinical diagnosis, such as analyzing magnetic resonance imaging (MRI) using texture parameters obtained from the distribution of gray levels in the image. The aim of this study was to verify whether the gray-level co-occurrence matrix (GLCM), a type of texture analysis method, applied to brain MRI, was able to provide parameters that could help differentiate between healthy individuals (HC) and individuals with schizophrenia with (AVH+) and without (AVH-) auditory hallucinations. Using the contrast and entropy parameters obtained from the GLCM, we were unable to find significant differences between healthy and pathological individuals, nor among the patients with schizophrenia.

Keywords: Schizophrenia; Texture Analysis; Magnetic Resonance Imaging.

1. Introduction

According to the World Health Organization, schizophrenia is a psychiatric disorder that affects more than 20 million people worldwide (1). The disorder can be diagnosed through the presentation of both positive and negative symptoms, as defined in the Diagnostic and Statistical Manual of Mental Disorders (DSM-5), provided that the required criteria, divided into sections A to F, are met (2).

Criterion A, known as the active symptom phase, defines five symptoms—delusions, hallucinations, disorganized speech, catatonic or grossly disorganized behavior, and negative symptoms such as blunted affect, apathy, and motor impairment—of which at least two must be present for a minimum of one month. Criterion B refers to the patient's social or occupational dysfunction as a consequence of the disturbances caused by active symptoms. Criterion C establishes six months as the minimum duration of disturbance resulting from active symptoms or their milder expressions, such as in prodromal and residual phases. Criteria D and E ensure that the period of disturbance is not attributable to schizophrenia in cases of schizoaffective disorders, mood disorders, such as bipolar disorder and depression, or substance abuse. Finally, Criterion F allows the diagnosis of schizophrenia in individuals on the autism spectrum when apparent symptoms such as hallucinations and delusions are present for at least one month (2).

The series of criteria and the variability in the manifestation of symptoms among patients highlight the challenges in accurately diagnosing schizophrenia. This often leads to delayed diagnoses, which are associated with treatment resistance and, consequently, reduced effectiveness due to the deterioration of cognitive, social, self-care, mobility, and daily living skills (3). For this reason, several research fields have been dedicated to developing and improving alternative methods to support schizophrenia diagnosis. Among these is the technique of texture analysis, applied to magnetic resonance imaging (MRI). Texture analysis consists of several image-processing methods that extract texture-related parameters from images, i.e., patterns formed by gray levels (4). These methods have been successfully used to differentiate healthy from pathological tissues (4).

Application of texture analysis to brain MRI of patients with schizophrenia is not novel. Kovalev et al. used anisotropy of the three-dimensional orientation histogram to distinguish between patients with schizophrenia and healthy controls using T2-weighted MRI, and a generalized co-occurrence matrix to find the areas responsible for this difference, which they found were located on the cortical surface over the tissue volume that constitutes the widening of the cerebral sulci (5). Ganeshan and colleagues used a Laplacian of Gaussian filter to quantify gray matter and white matter (WM) textural abnormalities associated with schizophrenia. They found that gray matter texture features best differentiated patients from controls (6). Radulescu and colleagues used the same texture method as Ganeshan et al., together with voxel-based morphometry (VBM), and found significant differences between individuals with schizophrenia and controls at the fine spatial scale (around 2mm), and correlation of texture parameters with the volumes of the hippocampus, amygdala, and cerebellum for the patients (7). Latha and Kavitha used geometrical and Laws texture features to investigate brain changes in schizophrenia patients and found that these features could be used as a diagnostic aid (8). Korda and colleagues investigated deep learning applied to gray-level co-occurrence matrix (GLCM) maps of non-segmented MRI to distinguish schizophrenia patients, major depression patients, and controls, with limited success (9,10). Carrasco-Poves et al. used several statistical texture features from the GLCM, gray-level run-length matrix,

gray-level size zone matrix, and neighborhood gray-tone difference matrix, extracted from MRI and positron emission tomography (PET) images for the same purpose, and obtained good results for classifying schizophrenia (11). More recently, Ding et al. used texture networks based on the GLCM and found structural heterogeneity and complex dysconnectivity specific to schizophrenia patients (12). Another recent study applied classical machine learning algorithms to local binary patterns and fast Fourier transform features and achieved good classification results for discriminating between schizophrenia patients and controls (13).

Despite all the studies aforementioned, we have found no studies attempting to use texture analysis to discriminate among schizophrenia patients with different symptoms. Therefore, this study aimed to apply texture analysis to MRI scans of healthy individuals (HC) and patients with schizophrenia, with the latter divided into two subgroups: patients with schizophrenia experiencing auditory verbal hallucinations (AVH+) and patients with schizophrenia without auditory verbal hallucinations (AVH–) (14). The aim was to assess tissue differences among the groups based on the texture parameters extracted from each image. We intended to establish correlations between schizophrenia, the manifestation of auditory hallucinations, and tissue alterations.

2. Materials and Methods

2.1. Subjects

The data used for analysis were obtained from the OpenNeuro platform and collected for the study "Brain correlates of speech perception in schizophrenia patients with and without auditory hallucinations" (15). The sample comprised 3D structural T1-weighted MRIs, acquired with a 3T Philips Ingenia Scanner using Fast Field Echo (FFE) and TR = 9.90ms; TE = 4.60ms; Flip angle = 8°; voxel size = 1 × 1mm^2; slice thickness = 1mm; number of slices = 180; FOV = 240 × 240mm^2, from 71 individuals selected through a screening process, which evaluated age range (18–65 years) (Table 1), IQ above 70, substance dependence, history of electroconvulsive therapy, mental disorders, and neurological trauma. In addition, patients were assessed regarding the presence of auditory hallucinations and their severity using the Psychotic Symptom Rating Scale. This selection resulted in the formation of the groups: HC (mean age = (40 ± 14) years; 28% female), with 25 participants, and AVH+ (mean age = (40 ± 13) years; 13% female) and AVH− (mean age = (45 ± 7) years; 30% female), with 23 patients each (15).

Table 1. Age, sex and group of the subjects of this study.

Subject-ID	Age	Sex	Group
Sub-01	47	Male	HC
Sub-02	36	Male	HC
Sub-03	43	Male	HC
Sub-04	25	Male	HC
Sub-05	52	Female	HC
Sub-06	23	Female	HC
Sub-07	38	Female	HC
Sub-08	22	Male	HC
Sub-09	57	Female	HC
Sub-10	36	Female	HC
Sub-11	32	Male	HC
Sub-12	51	Female	HC
Sub-13	21	Male	HC
Sub-14	26	Male	HC
Sub-15	21	Female	HC
Sub-16	20	Male	HC
Sub-17	51	Male	HC
Sub-18	31	Male	HC
Sub-19	60	Male	HC
Sub-20	53	Male	HC
Sub-21	42	Male	HC
Sub-22	58	Male	HC
Sub-23	33	Male	HC
Sub-24	64	Male	HC
Sub-25	53	Male	HC
Sub-26	38	Male	AVH-
Sub-27	31	Male	AVH-
Sub-28	43	Male	AVH-
Sub-29	38	Male	AVH-
Sub-30	45	Female	AVH-
Sub-31	43	Male	AVH-
Sub-32	55	Female	AVH-
Sub-33	41	Male	AVH-
Sub-34	51	Female	AVH-
Sub-35	48	Male	AVH-
Sub-36	42	Male	AVH-
Sub-37	41	Male	AVH-
Sub-38	45	Female	AVH-
Sub-39	41	Male	AVH-
Sub-40	50	Female	AVH-
Sub-41	61	Male	AVH-
Sub-42	43	Male	AVH-
Sub-43	58	Male	AVH-
Sub-44	47	Female	AVH-
Sub-45	37	Male	AVH-
Sub-46	53	Male	AVH-
Sub-47	48	Male	AVH-

Sub-48	35	Female	AVH-
Sub-49	44	Male	AVH+
Sub-50	37	Male	AVH+
Sub-51	40	Female	AVH+
Sub-52	32	Male	AVH+
Sub-53	25	Male	AVH+
Sub-54	32	Male	AVH+
Sub-55	31	Male	AVH+
Sub-56	52	Male	AVH+
Sub-57	19	Male	AVH+
Sub-58	34	Male	AVH+
Sub-59	60	Male	AVH+
Sub-60	44	Male	AVH+
Sub-61	52	Male	AVH+
Sub-62	24	Male	AVH+
Sub-63	48	Male	AVH+
Sub-64	44	Male	AVH+
Sub-65	66	Female	AVH+
Sub-66	64	Male	AVH+
Sub-67	20	Female	AVH+
Sub-68	42	Male	AVH+
Sub-69	32	Male	AVH+
Sub-70	39	Male	AVH+
Sub-71	41	Male	AVH+

Source: The Author (2026).

2.2. Methods

Image preprocessing was performed using SPM12 in MATLAB (version R2021a). First, the anterior commissure was defined, followed by segmentation, spatial normalization, and coregistration. During coregistration, the normalized MR images were resliced using the AAL FULL atlas masks as reference images to match their spatial grids. Anatomical structures were identified with the aid of the anatomical parcellation masks from the Automated Anatomical Labeling (AAL) atlas (16).

Subsequently, gray-level normalization was applied to the images in order to reduce the sparsity (zero entries) of the GLCMs. Accordingly, the intensity range was rescaled from 0–4095 to 0–31.

We used the final (gray-level normalized) image to construct GLCMs, which evaluate the co-occurrence distribution of paired pixel intensities. GLCM construction considers the intensity of a pixel and that of its neighbor, depending on the distance between them, and usually also on the direction among pixels. In this study, a 3D isotropic method was applied (17), and distances ranging from one to five voxels were considered, disregarding direction; i.e., all neighboring voxels in a cubic grid at the considered distance were taken into account to compute the matrix (see (17) for details). In this way, one GLCM was generated per distance for each brain structure selected for analysis, from which the texture parameters contrast and entropy were extracted.

The parameters contrast and entropy evaluate the contrast distribution and the disorder of the paired gray-level distribution of the image (or of the region of interest – ROI), respectively (18-20). Together, they provide complementary information on tissue heterogeneity. Given our goal of identifying structural differences between healthy and pathological individuals, as well as across patients' brains, we selected these parameters for initial investigation. Table 2 shows the mathematical formulae for these parameters, which use normalized GLCM elements.

Table 2. Mathematical expressions of the texture parameters used. $p(i,j)$ represents the non-normalized elements of a GLCM matrix.

Parameters	Mathematical expression
GLCM's normalized elements	$P(i,j) = \frac{p(i,j)}{\Sigma_{i,j} p(i,j)}$
Contrast	$CONT = \sum_{i}^{N_g} \sum_{j}^{N_g} P(i,j) \cdot (i-j)^2$
Entropy	$ENTR = -\sum_{i}^{N_g} \sum_{j}^{N_g} P(i,j) \cdot (log_{10}(P(i,j)))$

Source: The Author (2026).

Finally, we selected 18 pairs of homologous (left and right) brain structures from the AAL (16), including the inferior parietal cortex, bilateral superior frontal cortex, lateral and inferior prefrontal cortex, and the supplementary motor area. These are presented in Table 3, where the structures are listed along with their corresponding acronyms in the AAL.

Table 3. Analyzed anatomical structures and their acronyms in the AAL.

AAL Region	Anatomical Structure
Amygdala	Amygdala
Angular	Angular Gyrus
Frontal_Inf_Oper	Opercular Inferior Frontal Gyrus
Frontal_Inf_Orb	Orbital Inferior Frontal Gyrus
Frontal_Inf_Tri	Triangular Inferior Frontal Gyrus
Frontal_Mid	Middle Frontal Gyrus
Frontal_Mid_Orb	Orbital Middle Frontal Gyrus
Heschl	Heschl Gyrus
Hippocampus	Hippocampus
Parahippocampal	Parahippocampal Gyrus
Parietal_Inf	Inferior Parietal Lobe
Precuneus	Precuneus
Putamen	Putamen
Supp_Motor_Area	Supplementary Motor Area
SupraMarginal	Supramarginal Gyrus
Temporal_Pole_Sup	Superior Temporal Pole
Temporal_Sup	Superior Temporal Lobe
Thalamus	Thalamus

Source: The Author (2026).

The selection of brain structures was based on the original study (14), as they exhibit morphological alterations associated with schizophrenia. In particular, the Heschl gyrus and thalamus are involved in auditory processing, making them especially relevant for analyzing cases with auditory hallucinations.

Subsequently, another statistical analysis was performed to assess tissue differences among the groups in the selected regions. The Shapiro–Wilk test was applied to verify normality, followed by ANOVA for parametric data and the Kruskal–Wallis test, with Bonferroni correction (considering 18 AAL regions · 2 hemispheres), for non-parametric data, comparing the three groups. A significance level of 0.05 was adopted in all analyses.

3. Results

The statistical analysis began by assessing the influence of sex and age factors in order to account for them in the statistical model used to determine the distribution of the extracted texture parameters. Application of the ANOVA test for the age factor revealed similar mean values across groups. Therefore, age was determined to be irrelevant for the data analysis (Figure 1).

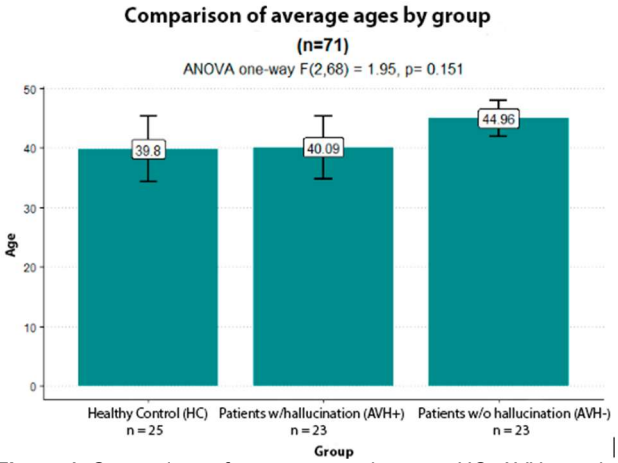


Figure 1. Comparison of average ages between HC, AVH+, and AVH- groups.

In contrast, the analysis of the sex factor revealed a limitation of the study due to the unequal distribution of men and women among the groups. The proportion of female participants showed a significant discrepancy in the AVH+ group (13%) compared with the others, AVH– (30%), and HC (28%). Therefore, the results of the analyses cannot be attributed solely to schizophrenia and auditory hallucinations; sex must be considered a relevant factor, and thus, the interpretation of the results cannot be generalized (Figure 2).

The Shapiro–Wilk test indicated non-normality, and the Kruskal-Wallis test was applied to assess differences in texture parameters among groups. We considered measurements statistically significant when the Kruskal–Wallis test returned $p < 0.05$.

The Kruskal-Wallis test revealed no statistically significant differences for the contrast and entropy parameters, and therefore no further statistical analyses were performed.

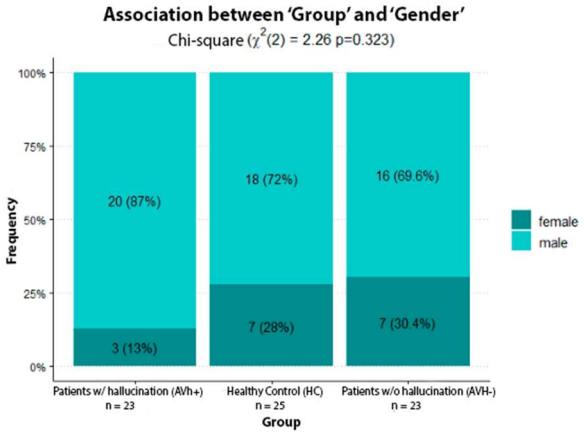


Figure 2. Comparison of sex distribution between HC, AVH-, and AVH+ groups.

4. Discussion

This study aimed to use texture parameters extracted from the GLCM applied to brain MRI to attempt to distinguish between two groups of schizophrenia patients (with and without auditory hallucinations) and a control group of healthy subjects. We focused on the contrast and entropy parameters obtained from the GLCM. The contrast parameter quantifies local gray-level variations among pixel pairs in the GLCM, while entropy quantifies their degree of randomness.

The results obtained revealed no significant differences between healthy and pathological individuals, nor among the patients with schizophrenia. The ANOVA test, applied to the age distribution of the participants, showed that age does not influence the results obtained for the contrast and entropy values. In contrast, Figure 2 presents the ratio of men to women participating in this study and reveals a gender discrepancy, especially in the AVH+ group, indicating an imbalance in our sample. Nevertheless, Aleman et al. reported a 1.42 risk ratio for the incidence of schizophrenia in men compared with women at a young age (21). The authors also discussed how the selection criteria used in the included studies may have limited women's representation. For example, age restrictions excluding individuals over 65 years of age may have overlooked an age group in which women may have a relatively higher incidence of schizophrenia, potentially influencing the reported sex difference.

5. Conclusion

The findings reveal limitations in this study. First, as discussed, texture analysis of magnetic resonance images based on the gray-level co-occurrence matrix was not effective in distinguishing healthy from pathological individuals. Nor was it able to identify tissue differences specifically associated with the presence of auditory hallucinations. Both results may reflect the relatively small sample size, and a larger sample might yield more robust findings. Another limitation was the imbalance between men and

women in each group analyzed, which may restrict the generalizability of the findings.

Moreover, using only two texture parameters (contrast and entropy) and one texture analysis method (GLCM) limits the ability to find results consistent with the aim of this study. Several other texture methods, including those used by Ganeshan et al., Radulescu et al., Latha and Kavitha, and Carrasco-Poves et al., might yield other interesting results if applied to this cohort.

Thus, we acknowledge the need to analyze the remaining texture parameters and to consider other methods for applying texture analysis. Furthermore, we must consider other limitations of this study, including sample size, gender imbalance among participants, and the lack of control over disease stage, and how these might affect the overall results.

Acknowledgments

This research was supported by Brazilian National Council for Scientific and Technological Development (CNPq), Grants 129110/2024-8, 306255/2024-3 and 408389/2024-9 (INCT-NeuroComp); São Paulo Research Foundation (FAPESP), Grants 2013/07559-3 (BRAINN) and 2024/00998-6 (CRISQuaM); Funding Authority for Studies and Projects (FINEP), Grant 2140/22 (DReANNs); and Brazilian Coordination for the Improvement of Higher Education Personnel (CAPES) - Finance Code 001.

References

1. WHO, “World Health Organization - Schizophrenia,” Newsroom, 2022. [Online]. Available: https://www.who.int/news-room/fact-sheets/detail/schizophrenia.
2. Tandon R, Gaebel W, Barch DM, Bustillo J, Gur RE, Heckers S, Malaspina D, Owen MJ, Schultz S, Tsuang M, Van Os J, Carpenter W. Definition and description of schizophrenia in the DSM-5. Schizophr Res. 2013, 150(1): 3-10. doi: 10.1016/j.schres.2013.05.028
3. Chen R, Liou TH, Miao NF, Chang KH, Yen CF, Liao HF, Chi WC, Chou KR. Using World Health Organization Disability Assessment Schedule 2.0 in people with schizophrenia: a 4-year follow-up. Eur Arch Psychiatry Clin Neurosci. 2020, 270(3):301-310. doi: 10.1007/s00406-019-01000-5
4. Castellano G, Bonilha L, Li LM, Cendes F. Texture analysis of medical images. Clinical Radiology 2004, 59(12):1061-1069. doi: 10.1016/j.crad.2004.07.008.
5. Kovalev VA, Petrou M, Suckling J. Detection of structural differences between the brains of schizophrenic patients and controls. Psychiatry Res. 2003, 124(3):177-89. doi: 10.1016/s0925-4927(03)00070-2
6. Ganeshan B, Miles KA, Young RC, Chatwin CR, Gurling HM, Critchley HD. Three-dimensional textural analysis of brain images reveals distributed grey-matter abnormalities in schizophrenia. Eur Radiol. 2010, 20(4):941-8. doi: 10.1007/s00330-009-1605-1
7. Radulescu E, Ganeshan B, Shergill SS, Medford N, Chatwin C, Young RC, Critchley HD. Grey-matter texture abnormalities and reduced hippocampal volume are distinguishing features of schizophrenia. Psychiatry Res. 2014, 223(3): 179-86. doi: 10.1016/j.pscychresns.2014.05.014
8. Latha M, Kavitha G. Segmentation and texture analysis of structural biomarkers using neighborhood-clustering-based level set in MRI of the schizophrenic brain. MAGMA 2018, 31(4): 483-499. doi: 10.1007/s10334-018-0674-z
9. Korda AI, Ruef A, Neufang S, Davatzikos C, Borgwardt S, Meisenzahl EM, Koutsouleris N. Identification of voxel-based texture abnormalities as new biomarkers for schizophrenia and major depressive patients using layer-wise relevance propagation on deep learning decisions. Psychiatry Research: Neuroimaging 2021, 313:111303. doi: 10.1016/j.pscychresns.2021.111303
10. Gan L, Wang L, Liu H, Wang G. Based on neural network cascade abnormal texture information dissemination of classification of patients with schizophrenia and depression. Brain Res. 2024, 1830:148819. doi: 10.1016/j.brainres.2024.148819
11. Carrasco-Poves A, Ruiz-Espana S, Brambilla CR, Neuner I, Rajkumar R, Ramkiran S, Lerche C, Moratal D. Analysis of New Biomarkers for the Study of Schizophrenia Following a Radiomics Approach on MR and PET Imaging. Annu Int Conf IEEE Eng Med Biol Soc. 2022. 2022:234-237. doi: 10.1109/EMBC48229.2022.9871543
12. Ding H, Zhang Y, Xie Y, Du X, Ji Y, Lin L, Chang Z, Zhang B, Liang M, Yu C, Qin W. Individualized Texture Similarity Network in Schizophrenia. Biological Psychiatry 2024, 96(3):176-187, doi: 10.1016/j.biopsych.2023.12.025
13. Tyagi A, Singh VP, Gore MM. Spatial and frequency domain-based feature fusion for accurate detection of schizophrenia using AI-driven approaches. Health Inf Sci Syst. 2025, 13(1): 32. doi: 10.1007/s13755-025-00345-7
14. Soler-Vidal J, Fuentes-Claramonte P, Salgado-Pineda P, Ramiro N, García-León MA, Torres ML, Arévalo A, Guerrero-Pedraza A, Munuera J, Sarró S, Salvador R, Hinzen W, McKenna P, Pomarol-Clotet E, Brain correlates of speech perception in schizophrenia patients with and without auditory hallucinations. PLoS ONE 2022a, 17(12): e0276975. doi: 10.1371/journal.pone.0276975
15. Soler-Vidal J, Fuentes-Claramonte P, Salgado-Pineda P, Ramiro N, García-León MA, Torres ML, Arévalo A, Guerrero-Pedraza A, Munuera J, Sarró S, Salvador R, Hinzen W, McKenna P, Pomarol-Clotet E. Brain correlates of speech perception in schizophrenia patients with and without auditory hallucinations. OpenNeuro 2022b, [Dataset] doi: 10.18112/openneuro.ds004302.v1.0.1
16. Tzourio-Mazoyer N, Landeau B, Papathanassiou D, Crivello F, Etard O, Delcroix N, Mazoyer B, Joliot M. Automated anatomical labeling of activations in SPM using a macroscopic anatomical parcellation of the MNI MRI single-subject brain. Neuroimage 2002, 15(1): 273-89. doi: 10.1006/nimg.2001.0978
17. da Silveira, R.V., Li, L.M. & Castellano, G. Texture-based brain networks for characterization of healthy subjects from MRI. Sci Rep 13, 16421 (2023). https://doi.org/10.1038/s41598-023-43544-6.
18. Zwanenburg A, Vallières M, Abdalah MA, Aerts HJWL, Andrearczyk V, Apte A, Ashrafinia S, Bakas S, Beukinga RJ, Boellaard R, Bogowicz M, Boldrini L, Buvat I, Cook GJR, Davatzikos C, Depeursinge A, Desseroit MC, Dinapoli N, Dinh CV, Echegaray S, El Naqa I, Fedorov AY, Gatta R, Gillies RJ, Goh V, Götz M, Guckenberger M, Ha SM, Hatt M, Isensee F, Lambin P, Leger S, Leijenaar RTH, Lenkowicz J, Lippert F, Losnegård A, Maier-Hein KH, Morin O, Müller H, Napel S, Nioche C, Orlhac F, Pati S, Pfaehler EAG, Rahmim A, Rao AUK, Scherer J, Siddique MM, Sijtsema NM, Socarras Fernandez J, Spezi E, Steenbakkers RJHM, Tanadini-Lang S, Thorwarth D, Troost EGC, Upadhaya T, Valentini V, van Dijk LV, van Griethuysen J, van Velden FHP, Whybra P, Richter C, Löck S. The Image Biomarker Standardization Initiative: Standardized Quantitative Radiomics for High-Throughput Image-based Phenotyping. Radiology 2020, 295(2): 328-338. doi: 10.1148/radiol.2020191145
19. van Griethuysen, J. J. M., Fedorov, A., Parmar, C., Hosny, A., Aucoin, N., Narayan, V., Beets-Tan, R. G. H., Fillon-Robin, J. C., Pieper, S., Aerts, H. J. W. L. Computational Radiomics System to Decode the Radiographic Phenotype. Cancer Research 2017, 77(21): e104–e107. doi: 10.1158/0008-5472.CAN-17-0339
20. Haralick, R., Shanmugan, K., Dinstein, I; Textural features for image classification; IEEE Transactions on Systems, Man and Cybernetics 1973 (3):610-621
21. Aleman, A., Kahn, R. S., & Selten, J. P. (2003). Sex differences in the risk of schizophrenia: evidence from meta-analysis. Archives of General Psychiatry, 60(6), 565–571. https://doi.org/10.1001/ARCHPSYC.60.6.565

Contact:

Giuliana Fernanda Ricardo
Departamento de Raios Cósmicos e Cronologia (DRCC), Instituto de Física Gleb Wataghin, Universidade Estadual de Campinas
Rua Sérgio Buarque de Holanda, 777, Prédio A1, Cidade Universitária "Zeferino Vaz", Barão Geraldo, CEP 13083-859, Campinas, SP
g251096@dac.unicamp.br